ARF 2068-6

ARMOUR RESEARCH FOUNDATION OF ILLINOIS INSTITUTE OF TECHNOLOGY

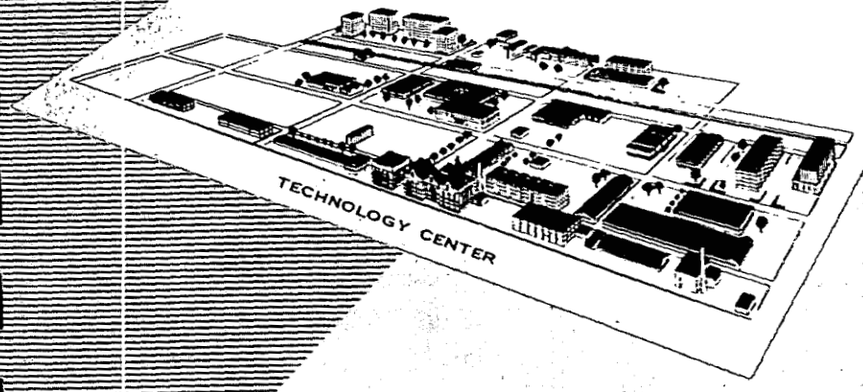

ARF Project B 068
Contract No. AT(11-1)-315

STUDIES OF ZIRCONIUM-IRON-TIN ALLOYS

Report No. 6, Final

RESEARCH FOR INDUSTRY

DISCLAIMER

This report was prepared as an account of work sponsored by an agency of the United States Government. Neither the United States Government nor any agency Thereof, nor any of their employees, makes any warranty, express or implied, or assumes any legal liability or responsibility for the accuracy, completeness, or usefulness of any information, apparatus, product, or process disclosed, or represents that its use would not infringe privately owned rights. Reference herein to any specific commercial product, process, or service by trade name, trademark, manufacturer, or otherwise does not necessarily constitute or imply its endorsement, recommendation, or favoring by the United States Government or any agency thereof. The views and opinions of authors expressed herein do not necessarily state or reflect those of the United States Government or any agency thereof.

DISCLAIMER

Portions of this document may be illegible in electronic image products. Images are produced from the best available original document.

ARMOUR RESEARCH FOUNDATION
of
ILLINOIS INSTITUTE OF TECHNOLOGY
Technology Center
Chicago 16, Illinois

AEC Research and Development Report

ARF 2068-6
Project No. B 068
Contract No. AT(11-1)-315

STUDIES OF ZIRCONIUM-IRON-TIN ALLOYS

Report No. 6, Final
July 1, 1958 - March 31, 1959

for

United States Atomic Energy Commission
Washington 25, D.C.

April 30, 1959

DISTRIBUTION LIST

Ames Laboratory 1
P.O. Box 14A, Station A
Ames, Iowa
Attention Dr. F. H. Spedding

Argonne National Laboratory 4
P.O. Box 299
Lemont, Illinois
Attention Dr. Hoylande D. Young

Atomics International 1
Div. North American Aviation Inc.
P.O. Box 309
Canoga Park, California
Attention Dr. Chauncey Starr

Battelle Memorial Institute 1
505 King Avenue
Columbus 1, Ohio
Attention Dr. H. W. Russell

Brookhaven National Laboratory 3
Technical Information Division
Documents Group
Upton, L.I., New York

Carbide & Carbon Chemicals Div. 2
K-25 Records Department
P.O. Box P
Oak Ridge, Tennessee

Dow Chemical Company 1
Rocky Flats Plant
P.O. Box 2131
Denver, Colorado

E. I. DuPont deNemours & Co. 2
Explosives Department
Atomic Energy Division
Wilmington 98, Delaware
Attention Document Custodian

General Electric Company 1
ANP Division
P.O. Box 132
Cincinnati 15, Ohio
Attention Director, Materials Res.

General Electric Company 2
Technical Information
P.O. Box 100
Richland, Washington
Attention Miss M. G. Freidank

Institute for the Study of Metals 1
University of Chicago
Chicago 37, Illinois
Attention Dr. Cyril S. Smith

Knolls Atomic Power Laboratory 3
P.O. Box 1072
Schenectady, New York
Attention Document Librarian

Los Alamos Scientific Laboratory 2
P.O. Box 1663
Los Alamos, New Mexico
Attention Report Librarian

Mound Laboratory 2
P.O. Box 32
Miamisburg, Ohio
Attention Central Files

National Advisory Committee for Aeronautics 1
Lewis Flight Propulsion Laboratory
21000 Brookpark Road
Cleveland 11, Ohio
Attention Director, Materials Res.

National Bureau of Standards 2
Connecticut Ave. & Van Ness St., N.W.
Washington 25, D.C.
Attention Dr. L. S. Taylor

Nuclear Metals, Inc. 1
155 Massachusetts Avenue
Cambridge 39, Massachusetts
Attention Dr. A. R. Kaufmann

Oak Ridge National Laboratory 4
P.O. Box P
Oak Ridge, Tennessee
Attention Central Files

DISTRIBUTION LIST (continued)

Sandia Corporation 1
Sandia Base
Document Division
Albuquerque, New Mexico

Sylvania Electric Products Inc. 2
Atomic Energy Division
P.O. Box 6
Bayside, L.I., New York
Attention Document Custodian

U.S. Atomic Energy Commission 2
1901 Constitution Ave., N.W.
Washington 25, D.C.
Attention Technical Library

U.S. Atomic Energy Commission 1
Division of Research
1901 Constitution Ave., N.W.
Washington 25, D.C.
Attention Chief, Metallurgy
& Materials Branch

U.S. Atomic Energy Commission 1
1901 Constitution Ave., N.W.
Washington 25, D.C.
Attention Chief, Patent Branch

U.S. Atomic Energy Commission 1
Hanford Operations Office
P.O. Box 550
Richland, Washington

U.S. Atomic Energy Commission 1
Idaho Operations Office
P.O. Box 1221
Idaho Falls, Idaho
Attention Technical Library

U.S. Atomic Energy Commission 3
New York Operations Office
70 Columbus Avenue
New York 23, New York
Attention Div. of Technical Information

U.S. Atomic Energy Commission 1
Oak Ridge Operations Office
P.O. Box E
Oak Ridge, Tennessee
Attention Dr. H. M. Roth

Dr. J. B. Johnson, Chief 1
Metallurgical Group, WCRR
Wright-Patterson Air Force Base
Ohio

U.S. Atomic Energy Commission 1
Schenectady Operations Office
P.O. Box 1069
Schenectady, New York
Attention Librarian

U.S. Department of the Navy 1
Bureau of Ships, Code 490
Washington 25, D.C.

U.S. Department of the Navy 1
Office of Naval Research, Code 423
Washington 25, D.C.

U.S. Naval Research Laboratory 1
Washington 25, D.C.
Attention Librarian

U.S. Department of the Army 1
Office of Ordnance Research
Box CM, Duke Station
Durham, North Carolina
Attention Dr. Peter Kosting

U.S. Department of the Air Force 1
Office of Scientific Research
Baltimore, Maryland
Attention Mr. C. Yost

University of California 3
Radiation Laboratory
Information Division
Room 128, Building 50
Berkeley 4, California
Attention Dr. R. K. Wakerling

University of California 1
Radiation Laboratory
P.O. Box 808
Livermore, California
Attention Librarian

DISTRIBUTION LIST (continued)

U.S. Atomic Energy Commission Technical Information Service P.O. Box 62 Oak Ridge, Tennessee	15
Westinghouse Electric Corporation Atomic Power Division P.O. Box 1468, Bettis Plant Pittsburgh 30, Pennsylvania Attention Librarian	2
Westinghouse Electric Corporation Bettis Atomic Power Division P.O. Box 1468 Pittsburgh 30, Pennsylvania Attention Dr. D. E. Thomas AlW Metallurgy Section	1
Attention Dr. K. M. Goldman	1
Attention Dr. J. Hino	1
Attention Mr. R. H. Fillnow	1
Attention Mr. F. L. Shubert	1
Oak Ridge National Laboratory P.O. Box X Oak Ridge, Tennessee Attention Dr. M. L. Picklesimer Metallurgy Division	1

STUDIES OF ZIRCONIUM-IRON-TIN ALLOYS

ABSTRACT

The areas in the vicinity of the intermetallic compounds of the zirconium-iron-tin system (i.e., $ZrFe_2$ and Zr_4Sn) were studied in detail between the temperatures 500° and 1100°C. The alloys were prepared from "Grade 1" iodide zirconium and high-purity iron and tin by nonconsumable-electrode arc melting techniques under an inert atmosphere. Specimens were encapsulated in Vycor and annealed at the prescribed temperatures followed by a water quench. Data were gathered through the use of metallographic, X-ray diffraction, visible incipient melting, and magnetic susceptibility techniques.

It was determined that Zr_4Sn (24.5w/o Sn) and θ (24.5w/o Sn and 7 to 8w/o Fe) are separate phases which are not in equilibrium with each other. These phases are believed to participate in two successive four-phase ternary peritectoid reactions between 980° and 900°C in conjunction with the phases α, β, and Zr_5Sn_3 as follows:

$$\beta + Zr_4Sn \rightleftharpoons \alpha + Zr_5Sn_3$$
$$\beta + Zr_5Sn_3 \rightleftharpoons \alpha + \theta$$

$ZrFe_2$ has been firmly established at its stoichiometric composition of 55w/o Fe, and it apparently has negligible solubility for tin. The specific magnetization of this ferromagnetic compound is of the order of 55 cgs at room temperature. Its Curie temperature is about 355°C.

TABLE OF CONTENTS

		Page
I.	INTRODUCTION	1
II.	MATERIALS	1
	A. Zirconium	1
	B. Preparation of Zirconium Melting Stock	3
	C. Iron and Tin	3
	D. Preparation of Iron and Tin Melting Stock	3
III.	EQUIPMENT AND EXPERIMENTAL PROCEDURES	3
	A. Arc Melting of Alloys	3
	B. Heat Treatment	5
	C. Metallographic Techniques	9
	D. X-Ray Equipment and Techniques	9
	E. Analytical Procedures	9
	F. Visible Melting Studies	10
	G. Magnetic Susceptibility Studies	10
IV.	RESULTS AND DISCUSSION	13
	A. The Tin-Rich Compounds	13
	B. The Iron-Rich Compound	28
	C. Magnetic Susceptibility Studies	34
V.	SUMMARY	37
VI.	CONTRIBUTING PERSONNEL AND LOGBOOKS	38
REFERENCES		40

LIST OF ILLUSTRATIONS

		Page
1	Compositions of Zirconium-Iron-Tin Alloys	7
2	Faraday-Type Apparatus for Determining Magnetic Susceptibility	11
3	Specimen and Specimen Container in Magnetic Susceptibility Apparatus	12
4	A 4.05w/o Fe-24.47w/o Sn alloy annealed at 900°C for 313 hours + 1000°C for 96 hours and water quenched	14
5	A Partial Isothermal Section of the Zirconium-Iron-Tin System at 1100°C.	16
6	A Partial Isothermal Section of the Zirconium-Iron-Tin System at 1000°C.	17
7	A Partial Isothermal Section of the Zirconium-Iron-Tin System at 900°C	18
8	A Partial Isothermal Section of the Zirconium-Iron-Tin System at 800°C	19
9	A Partial Isothermal Section of the Zirconium-Iron-Tin System at 700°C	20
10	A 0.54w/o Fe-22.61w/o Sn alloy quenched from 900°C	23
11	A 2.02w/o Fe-24.53w/o Sn alloy quenched from 900°C	23
12	A 5.15w/o Fe-24.25w/o Sn alloy quenched from 900°C	23
13	An 8.05w/o Fe-24.67w/o Sn alloy quenched from 900°C.	23
14	A nominal 2.5w/o Fe-15w/o Sn alloy quenched from 600°C.	25
15	A nominal 5w/o Fe-15w/o Sn alloy quenched from 600°C	25
16	A Tentative Vertical Section of the Zirconium-Iron-Tin System at 90w/o Zr	26
17	A Tentative Partial Vertical Section of the Zirconium-Iron-Tin System at 0.5w/o Fe	27
18	A 49.83w/o Fe alloy quenched from 900°C.	33
19	A 54.81w/o Fe alloy quenched from 900°C.	33
20	A 53.81w/o Fe-0.52w/o Sn alloy quenched from 900°C	33
21	Specific Magnetization of $ZrFe_2$	35

LIST OF TABLES

		Page
I	Analysis of Grade 1 Zirconium Crystal Bar	2
II	Lot Analyses of Iron and Tin	4
III	Compositions of Zirconium-Iron-Tin Alloys	6
IV	Heat Treatments of Zirconium-Iron-Tin Alloys	8
V	X-Ray Diffraction Patterns of Zirconium-Tin and Zirconium-Iron-Tin Alloys	21
VI	Diffraction Pattern of Zr_4Sn	29
VII	Diffraction Pattern of the θ Phase	30
VIII	Magnetic Susceptibility of Zirconium-Iron-Tin Alloys	36

STUDIES OF ZIRCONIUM-IRON-TIN ALLOYS

I. INTRODUCTION

In accordance with Contract AT(11-1)-315 entitled "A Study of Zirconium-Base Alloys," further investigation of the zirconium-iron-tin system has been carried out. This work was part of the supplement to the contract entitled "Phase Diagram Studies."

In previous work a number of partial isothermal sections were determined between 500° and 1100°C for the zirconium-rich portion of this system up to the binary compounds $ZrFe_2$ (55w/o Fe) and Zr_4Sn (24.5w/o Sn).[1,2] In addition, the solubility of iron and tin in alpha-zirconium was investigated down to 200°C.[2] In the current program certain critical areas of the diagram were studied in detail in order to complete the determination.

Small ingots of new alloys were prepared by arc melting the highest purity materials available. Some alloys made during the earlier stages of the investigation were also used. Heat treatments were carried out at temperatures between 500° and 1100°C. Metallographic and X-ray diffraction techniques were used to examine the structures quenched from the various annealing treatments. Also incorporated were visible incipient melting studies and magnetic susceptibility measurements.

II. MATERIALS

A. Zirconium

Zirconium crystal bar, produced by the decomposition of a volatile iodide, was used for all these studies. High-purity, "Grade 1" hafnium-free material was supplied by the AEC. The manufacturer's analysis appears in Table I.

TABLE I

ANALYSIS OF GRADE 1 ZIRCONIUM CRYSTAL BAR

Element	Concentration, ppm
Al	<35
C	33
Cu	<25
Fe	27
Mg	<10
Ti	<25

B. Preparation of Zirconium Melting Stock

The zirconium crystal bar, as-received, was coated with a corrosion product from autoclave tests by which its grade designation is determined. The bars were sand-blasted lightly, pickled for 1 minute in a 20% HNO_3-5% HF aqueous solution, rinsed in water and acetone, and dried. The bars were rolled to about 1/32 in. strip. The strip was cut into 10 in. lengths and pickled and rinsed again. The material was sheared to approximately 1/4 in. squares, cleaned with acetone, and stored.

C. Iron and Tin

High-purity, gas-free iron was supplied by National Research Corporation. High-purity tin was received from the Vulcan Detinning Company. Typical analyses of these materials appear in Table II.

D. Preparation of Iron and Tin Melting Stock

The surface of the as-received iron bar was removed by taking small lathe cuts. It was then sliced into 3/4 in. thick pieces and cold-rolled to 0.050 in. sheet. The sheet was sand-blasted lightly, vigorously rinsed in acetone, dried, and bottled for storage in mineral oil to prevent oxidation prior to arc melting.

Hemispherical ingots of tin were cut in sections, cold-rolled to approximately 1/32 in. sheet strip, sheared, cleaned in acetone, and bottled for storage.

III. EQUIPMENT AND EXPERIMENTAL PROCEDURES

A. Arc Melting of Alloys

Alloys were prepared in a nonconsumable-electrode arc melting furnace. This furnace has been widely used for the preparation of titanium, vanadium, and zirconium alloys. A water-cooled copper crucible and a tungsten-

TABLE II

LOT ANALYSES OF IRON AND TIN

Element	Concentration, w/o
	Iron
N	<0.001
O	<0.02
H	<0.005
Al	<0.001
C	<0.005
Cr	<0.001
Co	<0.001
Cu	<0.001
Mn	<0.001
Mo	<0.001
Ni	<0.001
Si	<0.001
Sn	<0.01
Ti	<0.001
W	<0.001
	Tin
Fe	0.0020
Sb	0.0002
Pb	nil
Cu	nil

tipped electrode were employed. The material is placed in the crucible and rapidly melted under a protective atmosphere of helium or argon gas by striking the arc on a tungsten stud and then transferring it to the charge material. A drawing of the furnace and a description of general melting techniques have been published.[3] Control melts of unalloyed zirconium were prepared and checked for hardness and microstructure throughout the melting program.

A series of 38 alloys was prepared for study of the regions in the vicinity of the intermetallic compounds (i.e., $ZrFe_2$ and Zr_4Sn). The nominal and analyzed compositions are listed in Table III. Most of these compositions are plotted in Figure 1 as well. Also included in the figure are alloys prepared during the earlier work that are pertinent to this investigation. Analyzed compositions are denoted by closed circles.

B. Heat Treatment

As-cast ingots were annealed at 900°C for 313 hours in sealed Vycor bulbs, followed by quenching to room temperature. These ingots were subsequently broken and samples taken for metallographic and X-ray diffraction determinations. Additional heat treatments of selected alloys at other temperatures were carried out in the same manner. These are listed in Table IV.

For anneals at 900°C and above, a partial pressure of argon was admitted to prevent the bulbs from collapsing. Evacuation was sufficient for anneals at lower temperatures. Quenching was accomplished by breaking bulbs under cold water.

Resistance-type, porcelain tube furnaces, whose control was within ±3°C, were employed. Temperatures were measured twice daily with a calibrated thermocouple.

TABLE III

COMPOSITIONS OF ZIRCONIUM-IRON-TIN ALLOYS

Alloy No.	Iron, w/o		Tin, w/o	
	Nominal	Analyzed	Nominal	Analyzed
400	0.5		24.5	
401	1.0	1.01	24.5	23.42
402	1.5	1.53	24.5	23.58
403	0.5		25.0	
404	1.0		25.0	
405	1.5		25.0	
406	0.2	0.22	24.5	23.46
407	0.2		25.0	
408	0.3	0.33	24.5	22.92
409	0.3		25.0	
410	0.4	0.43	24.5	23.66
411	0.4		25.0	
412	0.5	0.54	24.5	22.61
413	0.5		25.0	
414	0.6		24.5	
415	0.6		25.0	
416	0.7		24.5	
417	0.7		25.0	
418	0.8	0.85	24.5	22.70
419	0.8		25.0	
420	54.0	53.81	0.5	0.52
421	54.0	54.02	1.0	1.10
422	55.0	55.50	0.5	0.54
423	55.0	55.01	1.0	0.96
424	2.0	2.04	25.0	25.21
425	2.0	2.02	24.5	24.53
426	3.0	3.20	24.5	24.40
427	3.0	3.17	25.0	25.16
428	4.0	4.05	24.5	24.47
429	4.0	4.19	25.0	24.35
430	5.0	5.13	24.5	24.25
431	5.0	5.21	25.0	25.29
432	6.0	6.00	24.5	24.97
433	6.0	5.93	25.0	25.25
434	7.0	7.23	24.5	24.60
435	7.0	7.08	25.0	24.79
436	8.0	8.05	24.5	24.67
437	8.0	7.92	25.0	25.79

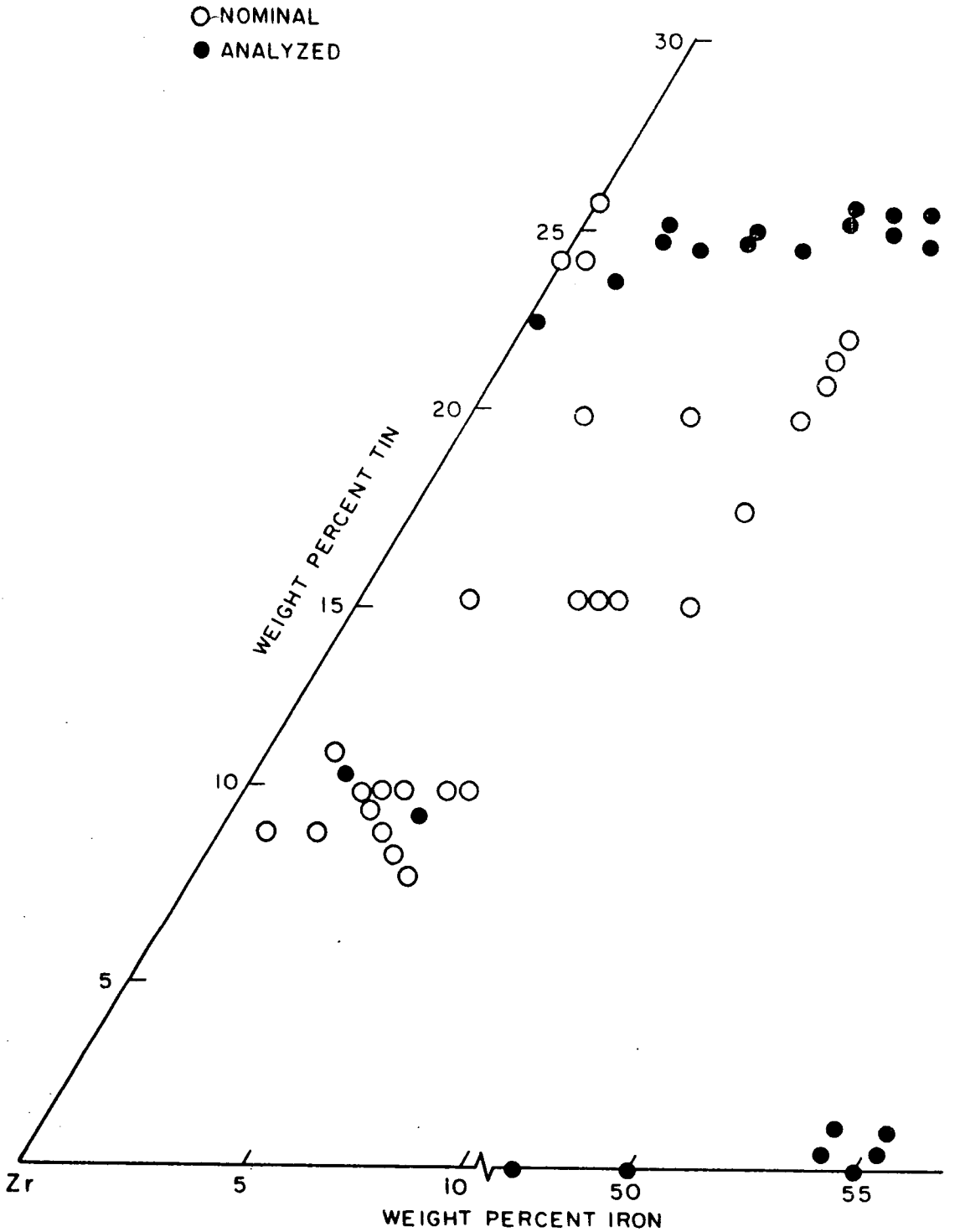

FIG. 1 - COMPOSITIONS OF ZIRCONIUM-IRON-TIN ALLOYS

TABLE IV

HEAT TREATMENTS OF ZIRCONIUM-IRON-TIN ALLOYS*

Temp, °C	Alloy No.	Time, hr
1100	401, 402, 404, 405 406, 407, 412, 413	96
1000	401, 402, 404, 405 406, 407, 412, 413 428, 433, 436	96
700	401, 402, 404, 405 406, 407, 412, 413 428, 433, 436	508
600	401, 402, 404, 405 406, 407, 412, 413	744
500	401, 402, 404, 405 406, 407, 412, 413 428, 433, 436	1008

* Prior anneal consisted of 313 hours at 900°C.

C. Metallographic Techniques

The first step in preparing samples for metallographic examination was to mount them in Bakelite. A belt sander employing 120-grit, silicon carbide abrasive rough-polished a preliminary flat surface. This was followed by the use of silicon carbide papers of grit Nos. 240, 320, 400, and 600. An alternate procedure incorporated a Lapmaster unit using Lapmaster 1900 lapping compound plus several passes on No. 600 paper. The final polishing operation involved two steps: polishing on airplane cloth impregnated with diamond paste in a kerosene vehicle, then on silk impregnated with "Linde B" synthetic sapphire, distilled water being the vehicle. The etchant employed was a solution of 20% HF and 20% HNO_3 in glycerine which was swabbed on the polished surface. Etching times ranged between 1 and 30 seconds.

D. X-Ray Equipment and Techniques

A 14-centimeter Debye-Scherrer powder camera and nickel-filtered copper radiation served for all X-ray work on this system. Minus 320 mesh powders were prepared by crushing heat-treated samples with a mortar and pestle. The samples were mounted in Pyrex capillaries and examined without stress-relief annealing.

E. Analytical Procedures

1. Iron

The alloy sample was dissolved in a mixture of HCl and HF. Then an aliquot was taken and the iron reduced with $H_2NOH \cdot HCl$. The sample was buffered with $NaC_2H_3O_2$, and the characteristic ferrous orthophenanthroline color developed by the addition of orthophenanthroline. After the adjustment of the sample to a standard volume, the optical density of the color complex and concentration was determined.

2. Tin

The zirconium sample is dissolved in a mixture of dilute HBF_4-H_2SO_4. The solution is diluted and HCl is added. Sn^{IV} is reduced to Sn^{II} with iron powder. Stannous tin is titrated with a standard iodine or iodate solution to the starch-iodine end point.[4]

F. Visible Melting Studies

Visible melting studies were made with a vacuum resistance furnace which has been described in detail.[5] Specimens supported on tungsten wires were heated rapidly until visible melting occurred. Temperatures were determined with an optical pyrometer calibrated against the melting points of several metals.

G. Magnetic Susceptibility Studies

Of the phases present in this portion of the zirconium-iron-tin system, only $ZrFe_2$ is ferromagnetic. Thus, it was considered possible to establish the $\alpha + \theta/\alpha + \theta + ZrFe_2$ phase boundary through magnetic susceptibility measurements by determining the presence or absence of the ferromagnetic phase in the nonferromagnetic matrix of an alloy. Earlier attempts using the apparatus available in these laboratories were unsuccessful.[2] Further studies to find this boundary were made by Professor P. W. Selwood* with the more sensitive and versatile apparatus at his disposal. The apparatus is of the Faraday type and can make measurements above and below room temperature. Figure 2 shows the entire experimental setup, and Figure 3 indicates how the alloy sample is suspended in the magnetic field. Descriptions of the techniques have been published.[6] The alloy compositions were selected to bracket the phase boundary as established by metallographic observation. The samples weighed from 0.5 to 1.0 grams and were those employed previously for metallographic observation.

* Department of Chemistry, Northwestern University, Evanston, Illinois.

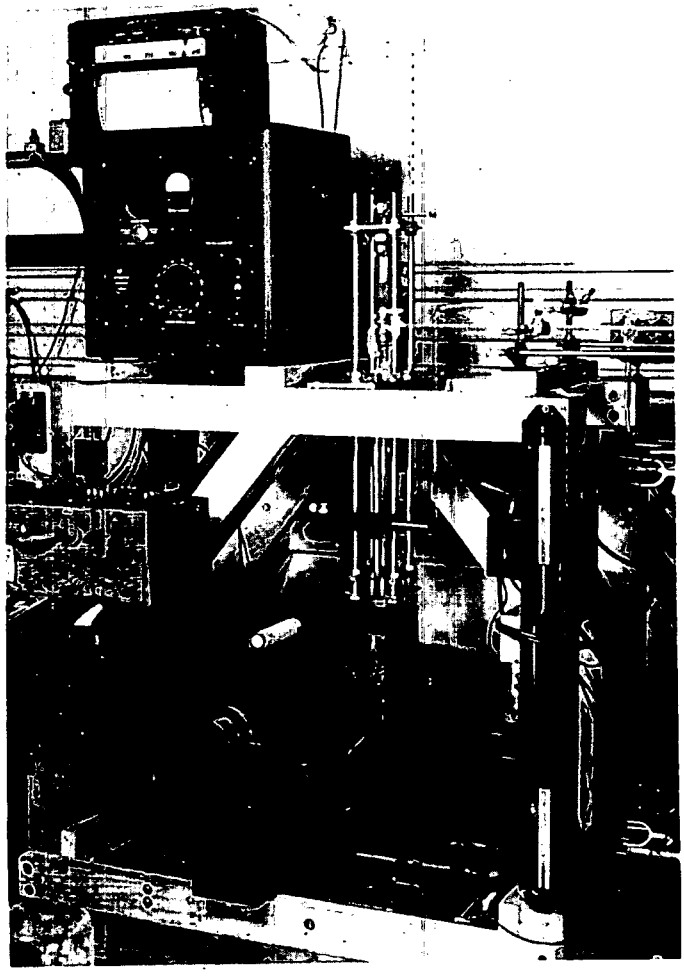

Neg. No. 17448

FIG. 2 - FARADAY-TYPE APPARATUS FOR DETERMINING MAGNETIC SUSCEPTIBILITY[6]

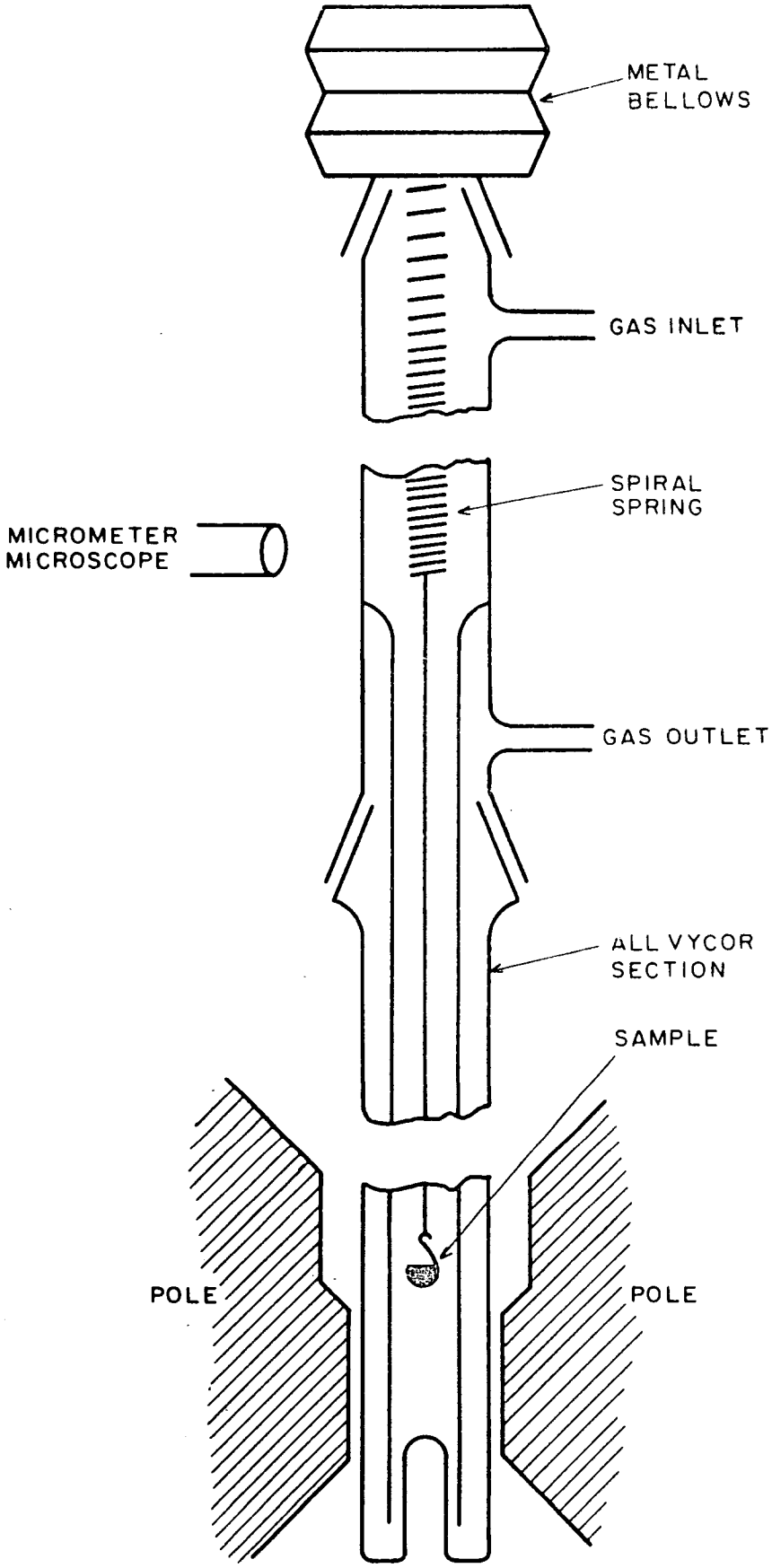

FIG. 3 - SPECIMEN AND SPECIMEN CONTAINER IN MAGNETIC SUSCEPTIBILITY APPARATUS[6]

IV. RESULTS AND DISCUSSION

A. The Tin-Rich Compounds

It was initially believed that the θ phase was a ternary modification of Zr_4Sn, being continuous to about 7 to 8w/o Fe at a constant tin composition of the order of 24.5w/o. This was based on the marked metallographic similarity of binary and ternary structures. Subsequent X-ray diffraction data, however, were not consistent with this view.[2]

The results of the current work have clarified this matter by establishing that Zr_4Sn and θ are distinctly different phases. It was also noted that they are not found in equilibrium with each other but, rather, are each in equilibrium with a third phase, Zr_5Sn_3.* The occasional appearance of this intermetallic compound in the first ternary microstructures examined in this region of the diagram gave rise to the belief that the Zr_5Sn_3 particles were the residual of an elevated-temperature (i.e., >1100°C) ternary reaction and not a stable phase. This had been observed in binary zirconium-tin structures in this program as well as by McPherson and Hansen[7] and was attributed to the sluggish nature of peritectoid reactions. However, it was quite obvious that Zr_5Sn_3 was stable when it persisted in microstructures of alloys after they were annealed for 313 hours at 900°C followed by 96 hours at 1000°C. An example is seen in Figure 4 of a 4.05w/o Fe-24.47w/o Sn alloy.**

---

* The stoichiometry of this phase remains tentative. McPherson and Hansen[7] believed it to be Zr_3Sn_2 (46.5w/o Sn) while Pietrokowsky[8] claimed the phase appeared at 43.8w/o Sn and was thus Zr_5Sn_3. The latter indexed the compound as a hexagonal $D8_8$ structure of the Mn_5Si_3 type having a = 8.461 Å, c = 5.795 Å, c/a = 0.685. Nowotny and Schachner[9] reported a compound in the composition interval $ZrSn_{0.55\pm0.05}$ (39.1 to 43.8w/o Sn) of the $D8_8$ structure.

** Analyzed compositions unless otherwise noted.

Neg. No. 17945 X 500

Fig. 4

A 4.05w/o Fe-24.47w/o Sn alloy annealed at 900°C for 313 hours + 1000°C for 96 hours and water quenched. Zr_5Sn_3 surrounded by θ peritectoid walls + transformed β.

Etchant: 20% HF, 20% HNO_3 in glycerine.

Additional four-phase ternary reactions must be inferred to account for the phase relations now observed at 1000°C (and higher) and 900°C (and lower). It is seen that α is introduced to the system at about 980°C by the binary peritectoid reaction:[7]

$$\beta + Zr_4Sn \rightleftharpoons \alpha$$

It is proposed that two successive four-phase ternary peritectoid transformations follow the above reaction, i.e.,

$$\beta + Zr_4Sn \rightleftharpoons \alpha + Zr_5Sn_3 \qquad [1]$$

$$\beta + Zr_5Sn_3 \rightleftharpoons \alpha + \theta \qquad [2]$$

The new phase fields are shown in a series of partial isothermal sections for 1100° to 700°C in 100-degree intervals (Figures 5 to 9, respectively) documented with data points. Except for a diminishing α field with decreasing temperature, the isotherms at 600°C and lower are identical with the 700°C section.

To illustrate further the above phase relations, X-ray diffraction data of three binary and four ternary alloys are presented in Table V. The X-ray film of 46.7w/o Sn alloy was obtained from the files of the earlier work of McPherson and Hansen[7] and was re-evaluated in order to be able to compare relative intensities with the other patterns. The structures of some of these alloys contained some α at their equilibration temperatures. Where diffraction lines could be positively identified as belonging only to α they were eliminated for the sake of clarity. This left the lines of Zr_4Sn, Zr_5Sn_3, or θ. The quenched structures of the ternary alloys are found in Figures 10 to 13. The comparison of d values shows rather clearly that Zr_4Sn is only present in the 0.54w/o Fe-22.61w/o Sn alloy of the ternary alloys. Additional evidence indicates it remains stable to about 1w/o Fe (at this high tin content).* Beyond

---

* It was also noted iron solubility in Zr_4Sn, if any, must be <0.22w/o.

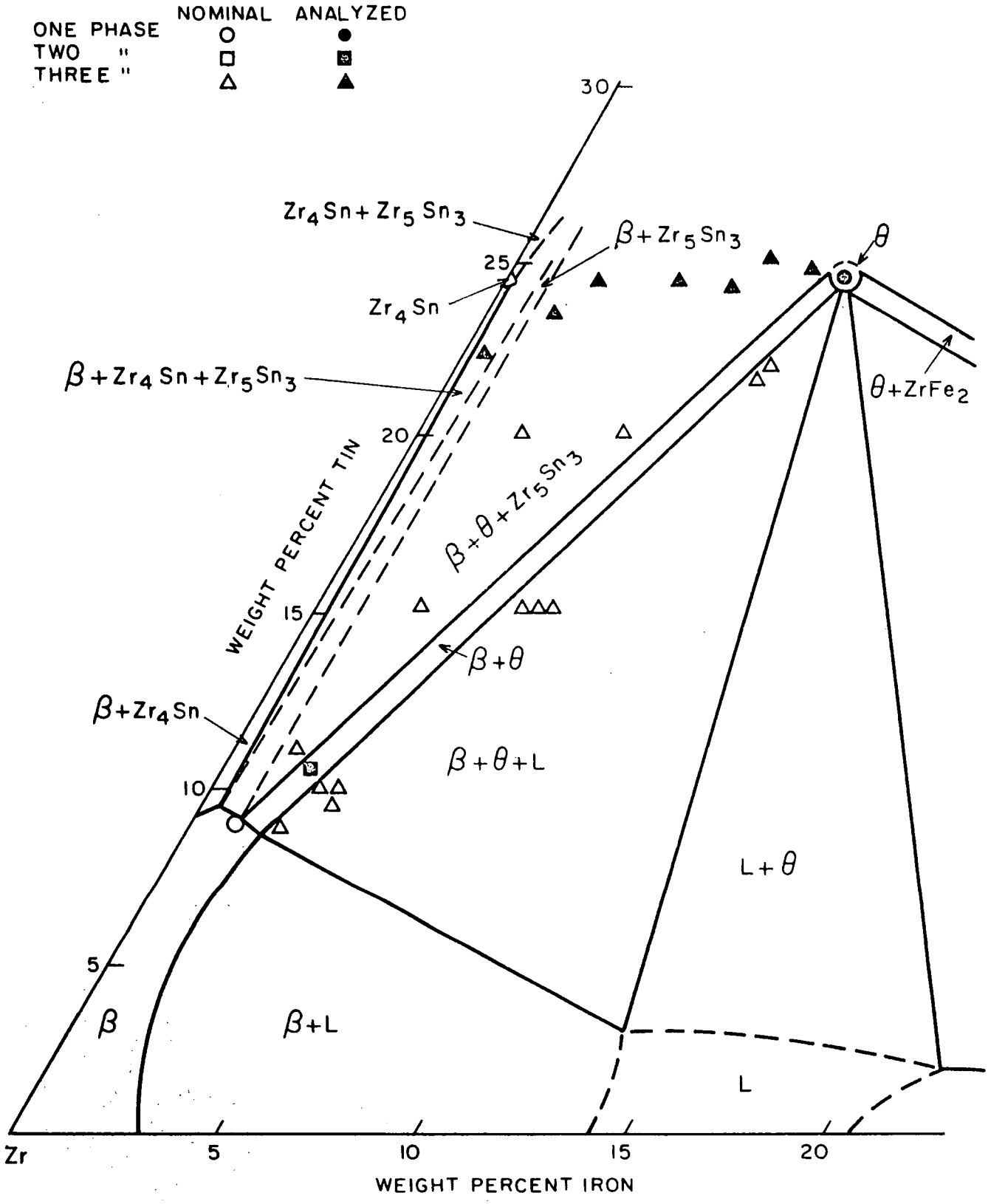

FIG. 5 - A PARTIAL ISOTHERMAL SECTION OF THE ZIRCONIUM-IRON-TIN SYSTEM AT 1100°C

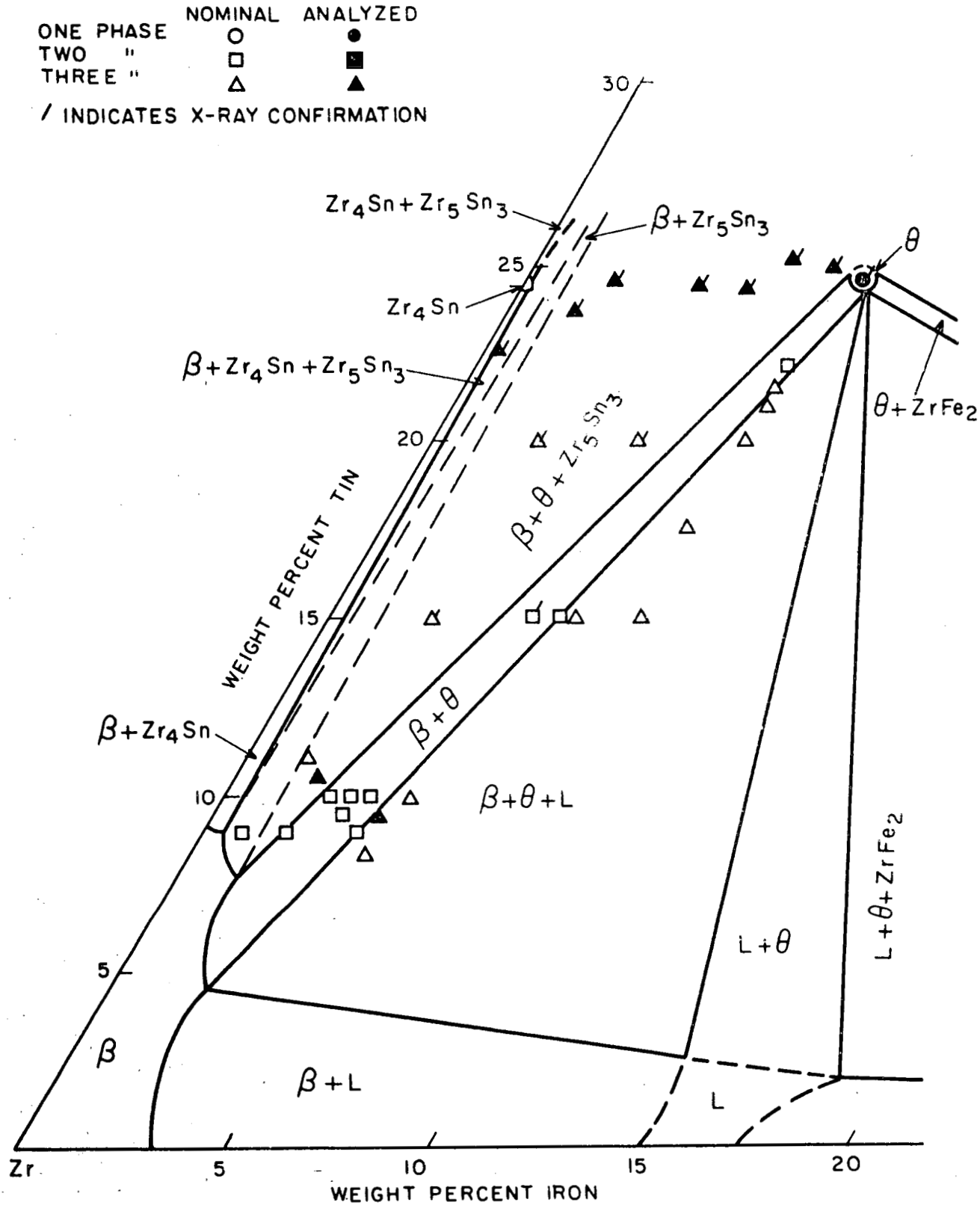

FIG. 6 - A PARTIAL ISOTHERMAL SECTION OF THE ZIRCONIUM-IRON-TIN SYSTEM AT 1000°C

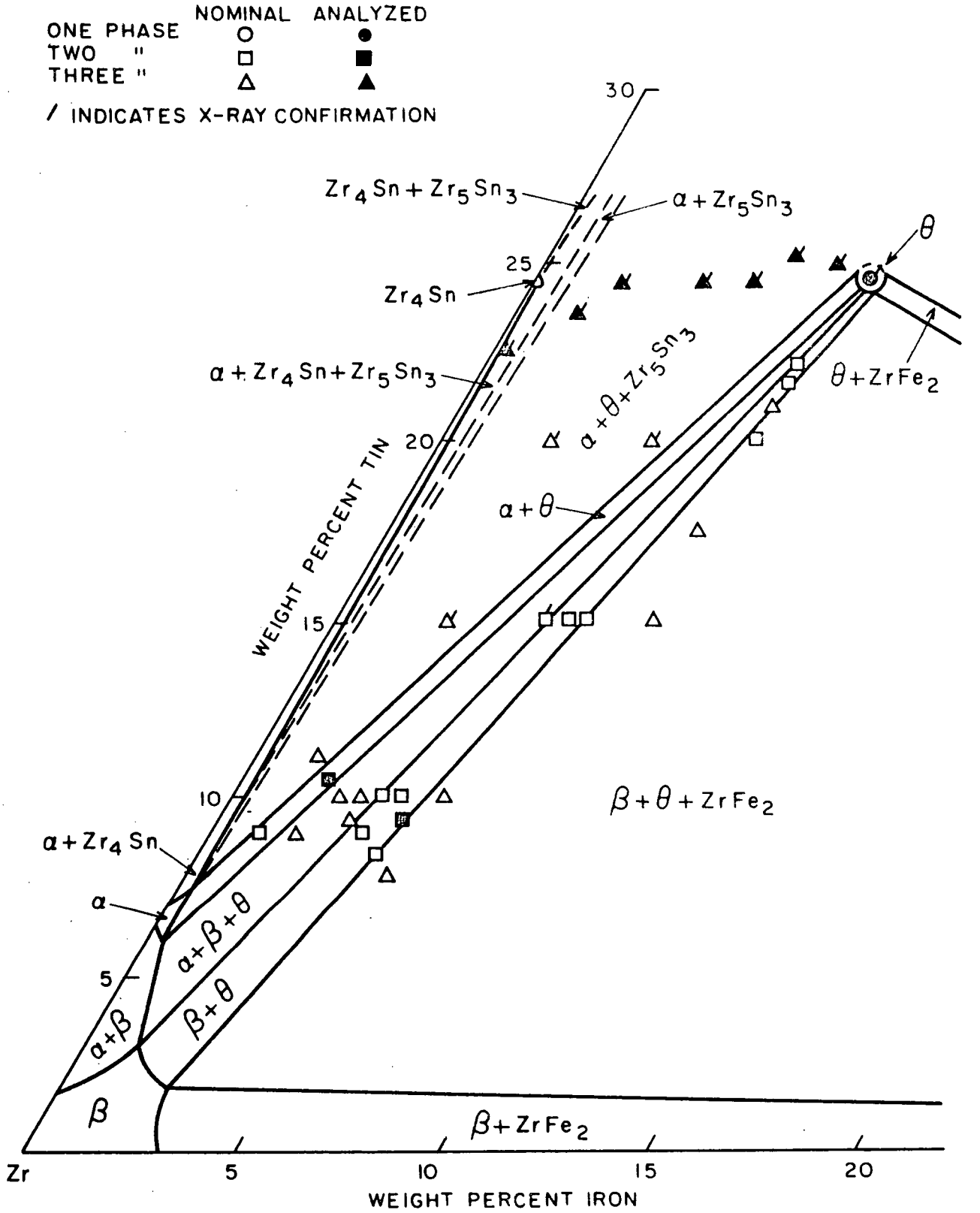

FIG. 7 - A PARTIAL ISOTHERMAL SECTION OF THE ZIRCONIUM-IRON-TIN SYSTEM AT 900°C

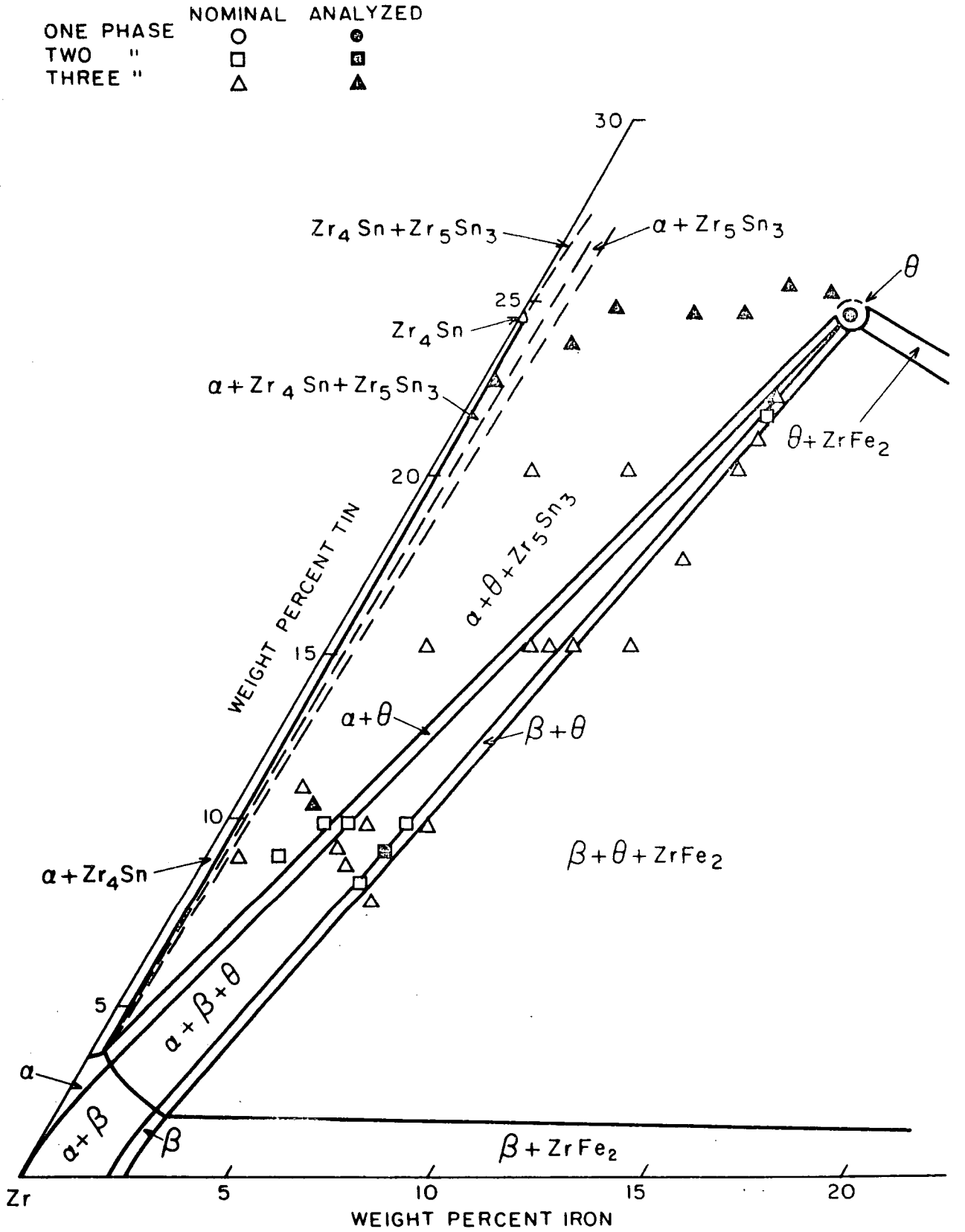

FIG. 8 - A PARTIAL ISOTHERMAL SECTION OF THE ZIRCONIUM-IRON-TIN SYSTEM AT 800 °C

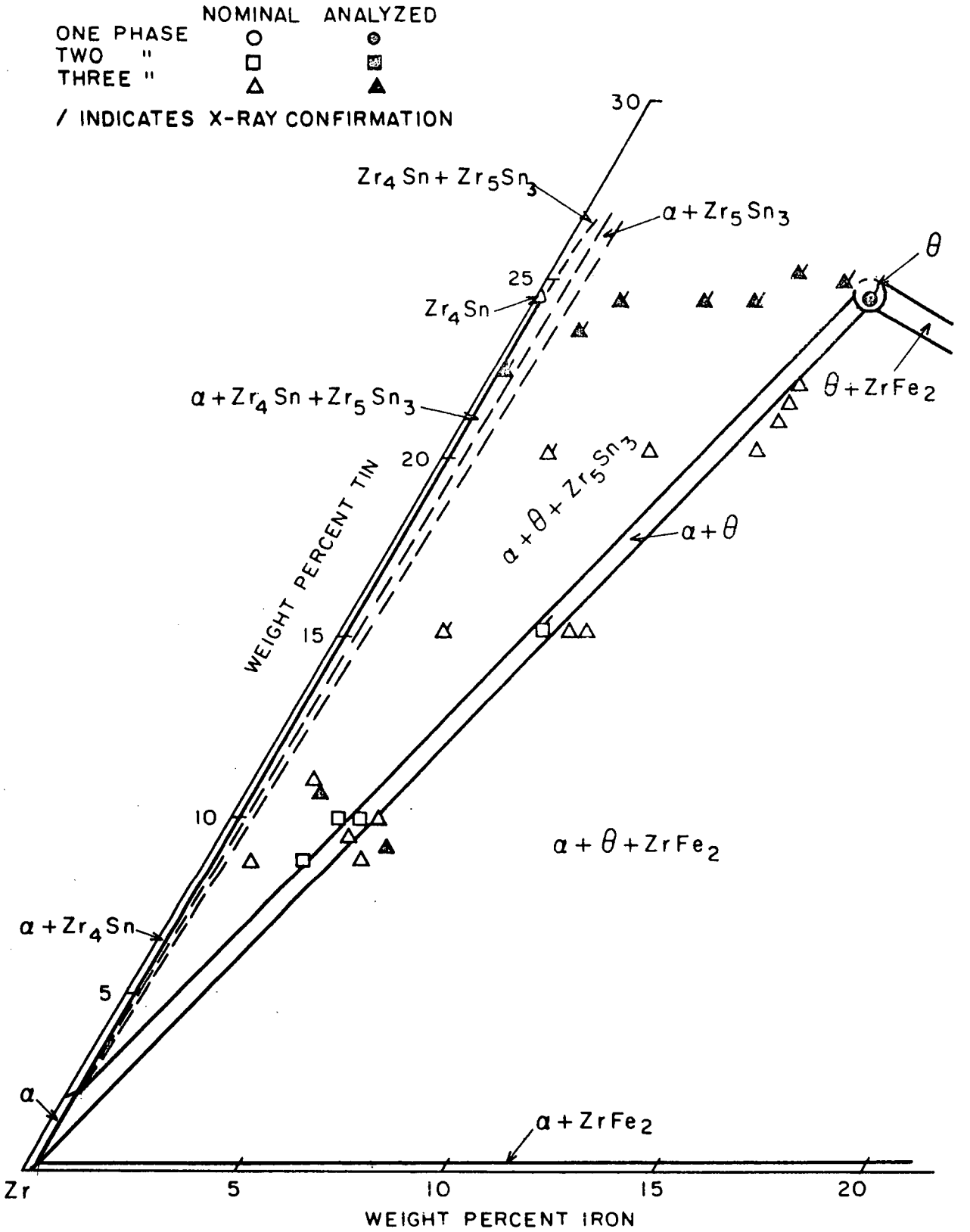

FIG. 9 - A PARTIAL ISOTHERMAL SECTION OF THE ZIRCONIUM-IRON-TIN SYSTEM AT 700°C

TABLE V

X-RAY DIFFRACTION PATTERNS OF ZIRCONIUM-TIN AND ZIRCONIUM-IRON-TIN ALLOYS

Comp, w/o	24.5Sn*		26Sn*		46.7Sn**		0.54Fe-22.61Sn		2.02Fe-24.53Sn		5.13Fe-24.25Sn		8.05Fe-24.67Sn	
Annealing Temp, °C	900		900		947		900		900		900		900	
Quenched Structure	nearly 100% Zr_4Sn		$Zr_4Sn+Zr_5Sn_3$		nearly 100% Zr_5Sn_3		$Zr_4Sn+Zr_5Sn_3+\alpha$		$\theta+Zr_5Sn_3+\alpha$		$\theta+Zr_5Sn_3+\alpha$		θ	
	I	d	I	d	I	d	I	d	I	d	I	d	I	d
					1	8.37								
	1	6.31					1	6.31						
													1	5.75
	1	5.65					1	5.66						
													1	5.35
	1	5.15					1	5.15						
													1	4.99
													1	4.56
					2	4.22								
	1	4.01					1	4.01						
					2	3.41								
													1	3.95
	1	3.38					1	3.39						
			1	2.89	5	2.89			2	2.87	1	2.87		
	5	2.82	4	2.82			5	2.81						
			1	2.77	4	2.78	3	2.75	4	2.75	2	2.75		
									3	2.60	7	2.60	10	2.60
	9	2.52	10	2.51			9	2.53						
			5	2.50	10	2.50			10	2.49	8	2.50		
	1	2.45	3	2.45	8	2.45	1	2.45	10	2.44	9	2.43	7	2.45
			3	2.38	9	2.39	3	2.37	3	2.37	6	2.38		
	10	2.29	10	2.29	1	2.28	10	2.29	2	2.28	5	2.28	8	2.28
									1	2.08	5	2.08	7	2.08

TABLE V (continued)

Comp, w/o	24.5Sn*		26Sn*		46.7Sn**		0.54Fe-22.61Sn		2.02Fe-24.53Sn		5.13Fe-24.25Sn		8.05Fe-24.67Sn	
Annealing Temp, °C	900		900		947		900		900		900		900	
Quenched Structure	nearly 100% Zr_4Sn		$Zr_4Sn+Zr_5Sn_3$		nearly 100% Zr_5Sn_3		$Zr_4Sn+Zr_5Sn_3+\alpha$		$\theta+Zr_5Sn_3+\alpha$		$\theta+Zr_5Sn_3+\alpha$		θ	
	I	d	I	d	I	d	I	d	I	d	I	d	I	d
									1	2.03	1	2.03	3	2.04
			1	1.98	1	1.99			1	1.98	1	1.98		
					4	1.93								
			3	1.91					2	1.91			4	1.91
			3	1.71	4	1.72			2	1.70	1	1.70	5	1.72
											1	1.68	6	1.67
	2	1.62	1	1.62	3	1.62	2	1.63	1	1.61	1	1.61		
			1	1.58	4	1.58			1	1.58	2	1.58	3	1.58
	4	1.56	4	1.56	1	1.56	4	1.56	1	1.55	1	1.54		
	8	1.51	8	1.50			8	1.51	1	1.49	1	1.50	6	1.49
					4	1.45			2	1.45	2	1.44	9	1.44
	4	1.41	4	1.40			4	1.41	1	1.40				
			1	1.38	1	1.38	2	1.38	1	1.38	1	1.38	8	1.38
			1	1.36	4	1.36			1	1.36				
			1	1.31	4	1.32			2	1.31	1	1.31		
			1	1.28	3	1.29			1	1.28	1	1.28		
	4	1.26	2	1.26			4	1.26						
					4	1.25			2	1.24	1	1.24		
	6	1.23	4	1.23			6	1.23						
			1	1.18	1	1.19			1	1.19				

* Nominal composition.

** From work of McPherson and Hansen.[7]

Neg. No. 17542 X 500

Fig. 10

A 0.54w/o Fe-22.61w/o Sn alloy quenched from 900°C. A Zr_4Sn + Zr_5Sn_3 + α structure.

Neg. No. 17543 X 500

Fig. 11

A 2.02w/o Fe-24.53w/o Sn alloy quenched from 900°C. θ peritectoid walls surrounding Zr_5Sn_3 crystals plus θ + α matrix.

Neg. No. 17544 X 500

Fig. 12

A 5.15w/o Fe-24.25w/o Sn alloy quenched from 900°C. θ + Zr_5Sn_3 + α structure.

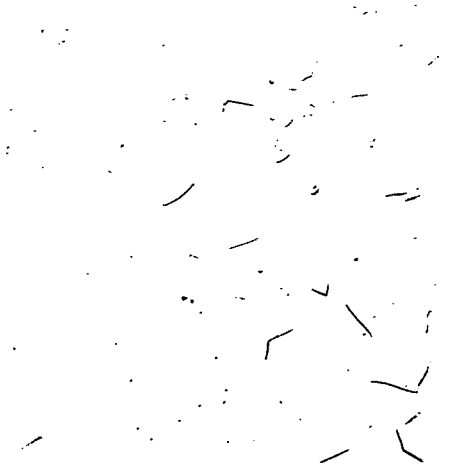

Neg. No. 17950 X 500

Fig. 13

An 8.05w/o Fe-24.67w/o Sn alloy quenched from 900°C. Single-phase θ structure (oblique light).

Etchant: 20% HF, 20% HNO_3 in glycerine.

this point θ becomes stable while Zr_5Sn_3 is still present. Between 7 and 8w/o Fe (and about 24.5w/o Sn) a single-phase θ structure is found. The relative intensities of the lines compared favorably with the relative amounts of phases observed metallographically.

The θ phase appears stable at all temperatures, and there is no indication of compositional change with temperature. An α + θ structure is seen in a 5w/o Fe-15w/o Sn* alloy (Figure 14) and an α + θ + Zr_5Sn_3 structure in a 2.5w/o Fe-15w/o Sn* alloy (Figure 15), both quenched from 600°C.

A vertical section at 90w/o Zr (parallel to the iron-tin system) was constructed to define the proposed phase transformations more clearly, and is presented in Figure 16. Besides passing through the planes of the two 4-phase reactions mentioned previously, the section also passes through the planes of two 4-phase reactions proposed in the earlier reports,[1,2] i.e.,

$$L \rightleftharpoons \beta + \theta + ZrFe_2 \text{ (between 935° and 930°C)} \qquad [3]$$
$$\beta + \theta \rightleftharpoons \alpha + ZrFe_2 \text{ (between 800° and 790°C)} \qquad [4]$$

A partial vertical section at 0.50w/o Fe (parallel to the zirconium-tin system) is shown in Figure 17. This was constructed to depict the phase fields below 700°C in proximity to the usual Zircaloy compositions.

The structure of Zr_4Sn was reported as being face-centered tetragonal with a = 7.645 Å, c = 12.461 Å; c/a = 1.63[7] but, when studying the indices assigned to the lattice spacings of this pattern,[10] it is obvious that they do not systematically obey the extinction rule for such a lattice (i.e., $h + k \neq 2n$, $h + l \neq 2n$ and $k + l \neq 2n$, where n is an integer). It is also apparent that the pattern would best fit c/a = 2.25 on the Hull-Davey chart for tetragonal lattices.** It is seen that if one were to transform the above

---

* Nominal composition.

** Attempts to fit the pattern on charts for other structures were unsuccessful.

Neg. No. 17546 X 500

Fig. 14

A nominal 2.5w/o Fe-15w/o Sn alloy quenched from 600°C. θ peritectoid walls surrounding Zr_5Sn_3 plus α + θ matrix.

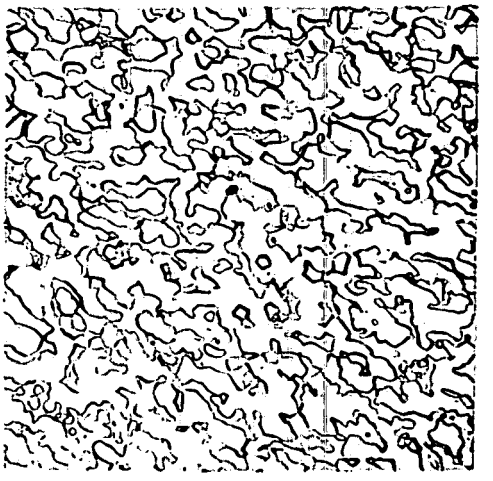

Neg. No. 17545 X 500

Fig. 15

A nominal 5w/o Fe-15w/o Sn alloy quenched from 600°C. θ + α structure.

Etchant: 20% HF, 20% HNO_3 in glycerine.

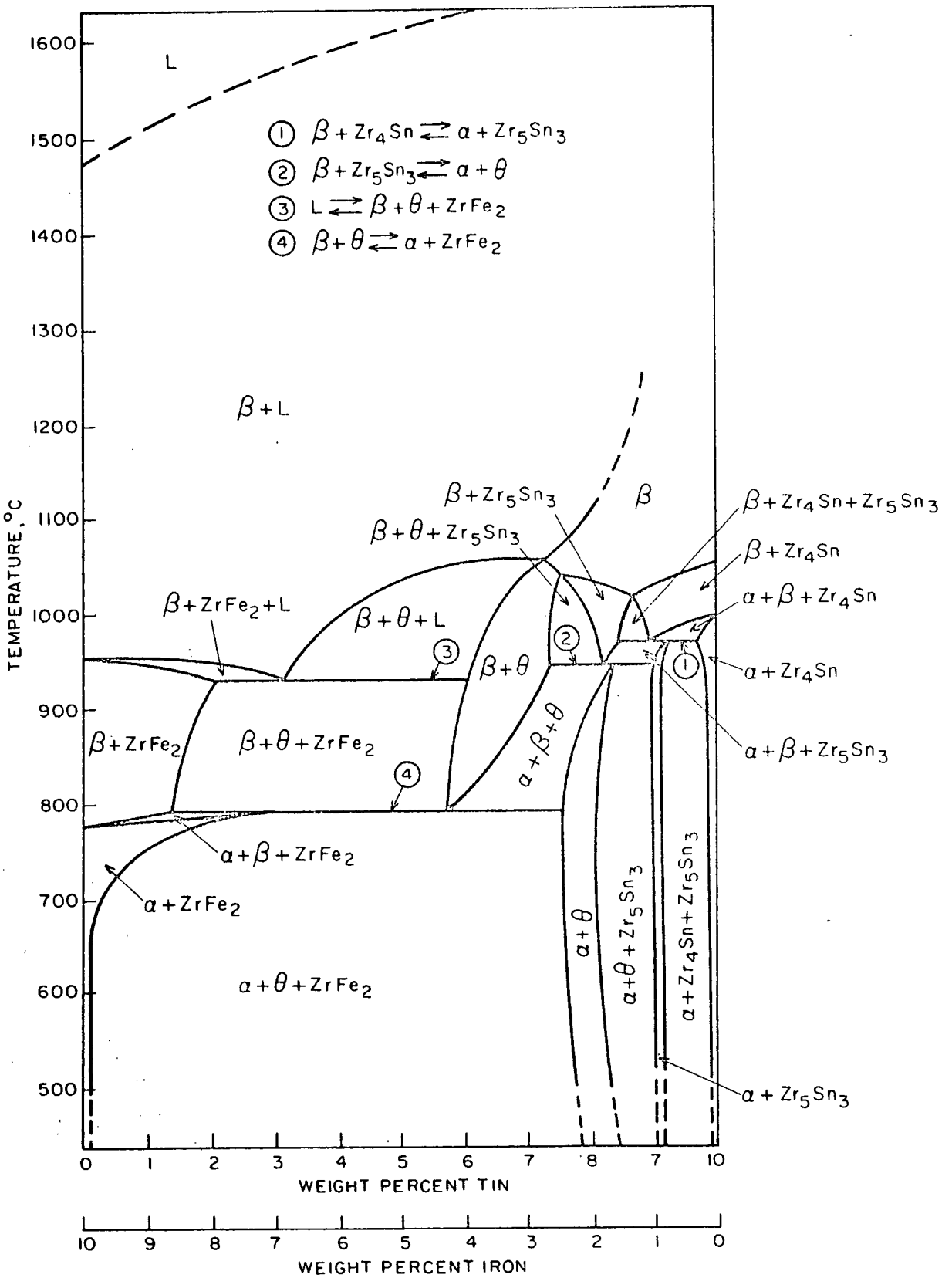

FIG. 16 - A TENTATIVE VERTICAL SECTION OF THE ZIRCONIUM-IRON-TIN SYSTEM AT 90w/o Zr

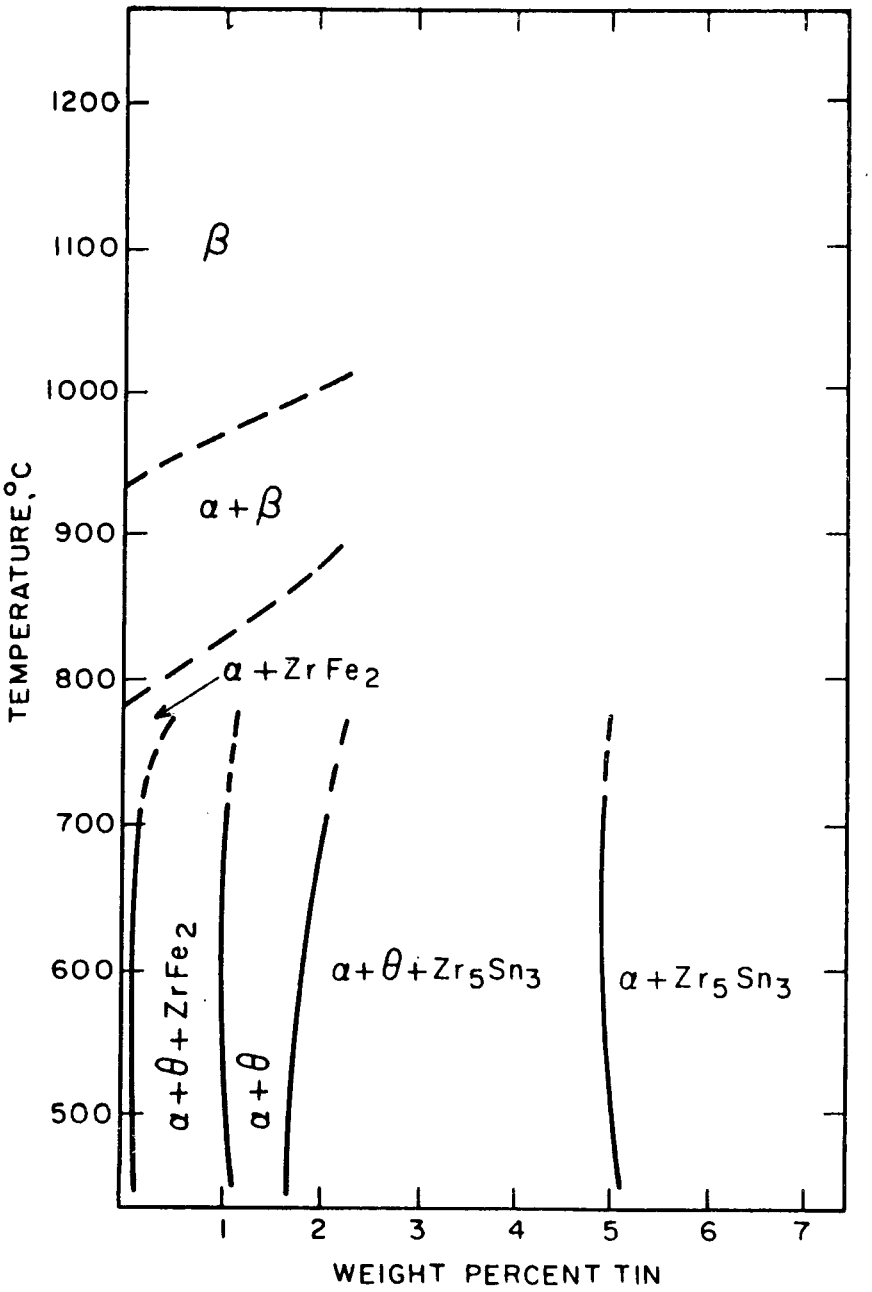

FIG. 17 - A TENTATIVE PARTIAL VERTICAL SECTION OF THE ZIRCONIUM-IRON-TIN SYSTEM AT 0.5w/o Fe

face-centered lattice to the body-centered variety, the latter c/a ratio, as well as the new lattice constants, are approximately in agreement with the required relationships for the transformation (i.e., $c/a_{FC} = 0.707\ c/a_{BC}$ where $a_{FC} = 1.414\ a_{BC}$ and $c_{FC} = c_{BC}$). However, once again, the corresponding extinction rule is not complied with (i.e., $h + k + l \neq 2n$, where n is an integer) nor is it possible to convert $(hkl)_{FC}$ to $(hkl)_{BC}$ for given lattice spacings and have them agree with the observed results.

The lattice spacings of the θ phase could also be fitted on the tetragonal chart at c/a = 1.65; however, much the same problem arose as was encountered with Zr_4Sn. The observed indices disclose no systematic agreement with either the body-centered or face-centered species. It is felt that within the limit of accuracy of the charts used, it is not possible to positively establish the structures at the present time.

The complete X-ray diffraction patterns of Zr_4Sn and θ appear in Tables VI and VII, respectively. Also included are the trial indices of both structures determined on the tetragonal Hull-Davey chart, as well as the calculated lattice spacings. The latter were based on the lattice constants determined by least-squares solutions using these indices.

B. <u>The Iron-Rich Compound</u>

Further study was made of the intermediate phase $ZrFe_2$. Wallbaum[10] identified the compound initially as $ZrFe_2$ with a C 15 ($MgCu_2$) structure, placing it at 55w/o Fe stoichiometrically. Hayes et al.[11] believed they found the phase at about 47.2w/o Fe and called it Zr_2Fe_3, but reverted to $ZrFe_2$ in the discussion of their paper.[12] Jordan and Duwez[13] confirmed Wallbaum's work while also finding the same single-phase structure to about 62.3w/o Fe or $Zr_{0.81}Fe_{2.19}$. In order to establish the ternary phase relations in this system

TABLE VI

DIFFRACTION PATTERN OF Zr_4Sn*

		Trial Tetragonal Indices	
I obs	d obs	hkl	d calc+
1	6.31	002	6.35
1	5.65	100	5.65
1	5.15	101	5.00
1	4.01	110	4.00
1	3.38	112	3.38
5	2.82	200	2.83
9	2.52	005	2.54
1	2.45	114	2.49
10	2.29	105	2.31
2	1.62	304	1.62
4	1.56	314	1.57
8	1.51	305	1.51
4	1.41	306	1.41
4	1.26	414	1.26
6	1.23	405	1.23
3	1.20		
6	1.05		
5	1.03		
4	0.996		
3	0.939		
1	0.927		
6	0.915		
1	0.850		
5	0.840		
4	0.831		
3	0.813		
4	0.781		
2	0.779		
5	0.774		

* Alloy: Zr-24.5w/o Sn (nominal);
heat treatment: 96 hr at 900°C-WQ.

\+ Based on: a = 5.651 Å
c = 12.693 Å
c/a = 2.25

TABLE VII

DIFFRACTION PATTERN OF THE θ PHASE*

		Trial Tetragonal Indices	
I obs	d obs	hkl	d calc+
1	5.75	100	5.85
1	5.35		
1	4.99	101	5.00
1	4.56		
1	3.95		
10	2.60	210	2.62
7	2.45	004	2.42
8	2.28	212	2.30
7	2.08	114	2.09
3	2.04	213	2.03
4	1.91	222	1.90
5	1.72	132	1.73
6	1.67	303	1.67
3	1.58	106/215	1.56
2	1.54		
6	1.49	116	1.50
9	1.44	401	1.45
8	1.38	330	1.38
2	1.33		
3	1.28		
3	1.24		
3	1.22		
4	1.17		
4	1.14		
1	1.10		
2	1.08		
4	1.06		
4	1.04		
6	1.01		
4	0.959		
3	0.951		
5	0.934		
1	0.925		
2	0.917		
2	0.901		
1	0.886		
1	0.871		
3	0.866		
1	0.859		

TABLE VII (continued)

I obs	d obs	Trial Tetragonal Indices hkl	d calc+
2	0.846		
1	0.840		
3	0.821		
3	0.811		

* Alloy: Zr-8.05w/o Fe-24.67w/o Sn; heat treatment: 313 hr at 900°C-WQ.

\+ Based on a = 5.851 Å
c = 9.653 Å
c/a = 1.65

the exact position of this phase had to be known, as well as its ternary solubility, if any.

X-ray diffraction evidence existed, obtained by Elliott[14] from an alloy of very nearly 55w/o Fe, which appeared to be completely single phase. This was confirmed in the present study with an alloy of 54.81w/o Fe. However, extra lines (attributable to α or β zirconium) were found in diffraction patterns of the 47.42 and 49.83w/o Fe alloy. In addition, a study of the melting characteristics of these alloys was made by suspending 47.42, 49.83, and 54.81w/o Fe samples on tungsten wires in a vacuum resistance furnace. These were then heated simultaneously until melting was observed. The two alloys with lower iron contents started melting first at some temperature above the eutectic. Complete melting occurred at the following temperatures: 47.42w/o Fe at 1590°C and 49.82w/o Fe at 1640°C. It is apparent that these were passing through a liquid + solid phase field. The 54.81w/o Fe alloy showed no signs of incipient melting prior to melting completely at one instant at 1650°C in the manner expected of a maximum-melting compound. To further substantiate assigning $ZrFe_2$ this stoichiometric composition, microstructures of the 49.83 and 54.81w/o Fe alloys annealed at 900°C for 313 hours are presented in Figures 18 and 19, respectively. The latter is nearly single-phase $ZrFe_2$ with very small amounts of retained β at the grain boundaries.

As suspected, there appears to be negligible solubility for tin in this compound. Metallography indicated three-phase structures in samples, quenched from all temperatures,* of alloys having about 55w/o Fe with as little as 0.5w/o Sn added (Figure 20). X-ray diffraction could identify θ when the alloys contained about 1w/o Sn.

---

* 1000°, 900°, 700°, and 500°C.

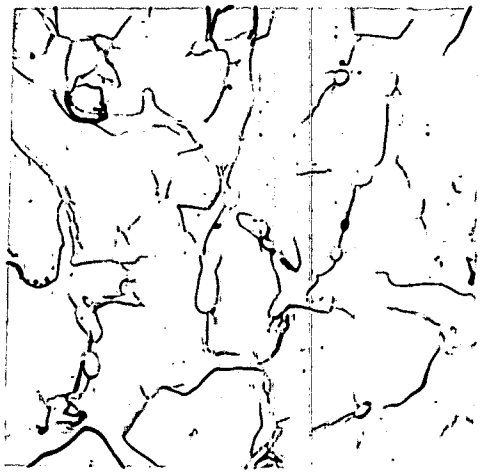

Neg. No. 17232 X 500

Fig. 18

A 49.83w/o Fe alloy quenched from 900°C. $ZrFe_2$ plus retained β at the grain boundaries.

Neg. No. 17233 X 500

Fig. 19

A 54.81w/o Fe alloy quenched from 900°C. Nearly 100% $ZrFe_2$ with some retained β.

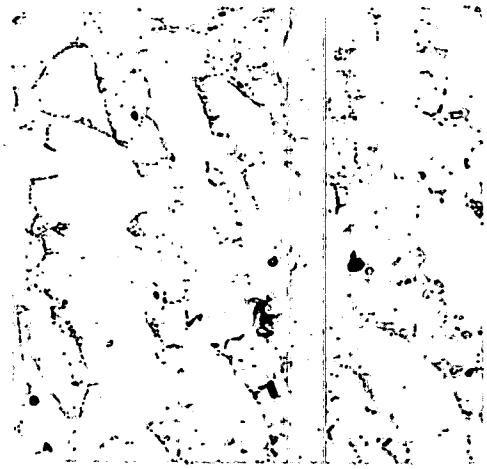

Neg. No. 17951 X 500

Fig. 20

A 53.81w/o Fe-0.52w/o Sn alloy quenched from 900°C. Primary $ZrFe_2$ crystals with β which is rejecting a θ precipitate.

Etchant: 20% HF, 20% HNO_3 in glycerine.

C. Magnetic Susceptibility Studies

Prior to making the susceptibility measurements on the alloys near the $\alpha + \theta/\alpha + \theta + ZrFe_2$ boundary the magnetic properties of $ZrFe_2$ were determined. A plot of the specific magnetization versus temperature of the compound is found in Figure 21. It is observed that the magnetic behavior of $ZrFe_2$ is quite similar to that of nickel, which has a specific magnetization of 55.1 cgs at room temperature and a Curie temperature of about 355°C. The Curie temperature is not defined as sharply as in the case of pure nickel. This could be due to the fact that the alloy, which has 54.81w/o Fe, is nearly, but not completely, single phase.

The susceptibility of paramagnetic and diamagnetic samples is independent of the magnetic field strength. However, when small amounts of ferromagnetic components are imbedded in a nonferromagnetic matrix, the apparent susceptibility of the combination may be shown to obey a relationship of the form:[15]

$$k_H = k_\infty + \frac{CM_s}{H}$$

where k_H is the apparent susceptibility at field strength H,
k_∞ is the true susceptibility of the matrix,
C is the concentration of the ferromagnetic component, and
M_s is its saturation magnetic moment.

The magnetic susceptibilities for the six samples studied are given in Table VIII. Data were obtained at 25° and -196°C. Measurements were made at 4460 and 6340 oersteds, and there was no observable dependence of susceptibility on field strength in any of the samples.

It would be expected to be able to estimate the upper limit of $ZrFe_2$ present; however, this may be subject to the following considerations. At

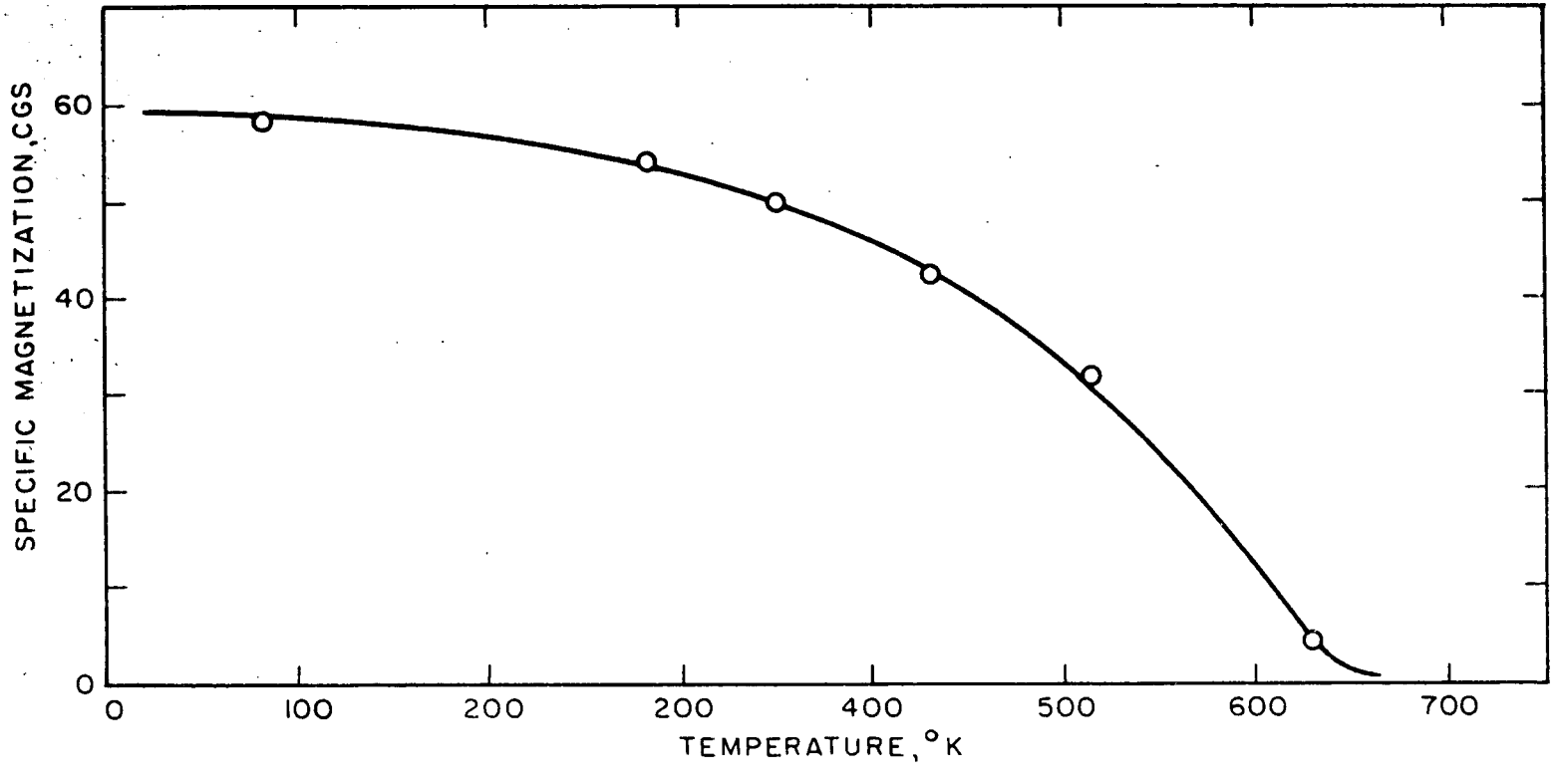

FIG. 21 - SPECIFIC MAGNETIZATION OF $ZrFe_2$

TABLE VIII

MAGNETIC SUSCEPTIBILITY OF ZIRCONIUM-IRON-TIN ALLOYS

Alloy No.	Analyzed Composition, w/o		Heat Treatment		Quenched Structure	Susceptibility (10^{-6} EMU/gm)	
	Iron	Tin	Time (hr)	Temp (°C)		at 25°C	at -196°C
47	1.07	3.14	744	600	$\alpha+\theta+ZrFe_2$	1.7	2.2
102	2.25	10.23	744	600	$\alpha+\theta+ZrFe_2$	0.8	1.8
185	4.07	9.06	744	600	$\alpha+\theta+Zr_5Sn_3$	0.9	1.7
341	0.047	0.047	1203	700	$\alpha+ZrFe_2(+\theta?)$	1.6	2.6
347	0.026	0.210	1203	700	$\alpha+ZrFe_2(+\theta?)$	1.1	2.3
350	0.051		1203	600	$\alpha+ZrFe_2$	2.0	3.3

4460 oersteds the susceptibility of $ZrFe_2$ from the data given would be 1.22 x 10^{-2} EMU/gram at 25°C, whereas at 6340 oersteds it would be 0.86 x 10^{-2}. Then 10^{-4} parts by weight of $ZrFe_2$ would have produced a field strength dependence of susceptibility amounting to about 0.36 x 10^{-6} units between the two fields. The apparatus was capable of detecting this, but no such dependence was found. The upper limit of ferromagnetic $ZrFe_2$ may therefore be set at about 0.01% However, according to the lever rule, there should be of the order of 0.1% $ZrFe_2$ in the 0.051w/o Fe alloy.

The following considerations could tend to raise this upper limit: First, the possibility that some dilution of the ferromagnetic phase occurs, a phenomenon which, in turn, would lower the Curie point. This would seem unlikely due to the narrow compositional range of the intermetallic compound and the extremely low solubility of iron in α-zirconium. Accordingly, no ferromagnetism was observed at -196°C while the paramagnetic susceptibility of each sample increased as the temperature was lowered, as would be expected. A second explanation would be that the size of the $ZrFe_2$ particles was too small to exhibit true ferromagnetism but became rather super-paramagnetic. In this case the apparent magnetization could be much smaller and strongly dependent on particle size. For particles in the range of 10 Å in diameter it is probable that several per cent of $ZrFe_2$ could escape detection even at -196°C. This seems to be quite reasonable since it is observed that particle size of $ZrFe_2$ changes considerably with small changes in iron content.

V. SUMMARY

Critical areas of the zirconium-iron-tin system were examined in detail and it was determined that:

(1) Zr_4Sn and θ are distinctly different phases. Zr_4Sn at 24.5w/o Sn has negligible solubility for iron, while the θ phase appears at the composition 24.5w/o Sn and 7 to 8w/o Fe.

(2) The above phases are not found in equilibrium with each other and are believed to participate in two successive four-phase ternary peritectoid reactions between 980° and 900°C in conjunction with the phases α, β, and Zr_5Sn_3, i.e.,

$$\beta + Zr_4Sn \rightleftharpoons \alpha + Zr_5Sn_3$$
$$\beta + Zr_5Sn_3 \rightleftharpoons \alpha + \theta$$

(3) The phase $ZrFe_2$ has been firmly established at its stoichiometric composition of 55w/o Fe. There appears to be negligible solubility for tin in this compound.

(4) Magnetic susceptibility techniques were unsuccessful in checking the $\alpha + \theta/\alpha + \theta + ZrFe_2$ phase boundary. However, it was found that $ZrFe_2$ has a specific magnetization of the order of 55 cgs at room temperature and a Curie temperature of about 355°C.

VI. CONTRIBUTING PERSONNEL AND LOGBOOKS

The following personnel contributed to the work:

W. A. Buknas	Heat Treatment
J. R. Dvorak	Metallography
D. W. Levinson	Supervisor
R. Moll	Arc Melting
H. F. Combs	Chemical Analysis
P. W. Selwood	Magnetic Susceptibility Measurements
C. R. Simcoe	Supervisor
B. J. Stang	Metallography
L. E. Tanner	Project Leader
M. Wright	Project Technician

Data relating to the work reported herein are recorded in ARF Logbook C-8111.

Respectfully submitted

ARMOUR RESEARCH FOUNDATION
OF ILLINOIS INSTITUTE OF TECHNOLOGY

Lee E. Tanner

L. E. Tanner
Associate Metallurgist

Charles R. Simcoe

Charles R. Simcoe
Supervisor
Nonferrous Metals Research

David W. Levinson

David W. Levinson
Assistant Director
Metals Research

REFERENCES

1. Tanner, L. E. and D. W. Levinson, "The System Zirconium-Iron-Tin," Contract No. AT(11-1)-315, Summary Report ARF 2068-4 (Aug. 12, 1957).

2. Tanner, L. E. and D. W. Levinson, "The System Zirconium-Iron-Tin," Contract No. AT(11-1)-315, Summary Report ARF 2068-5 (July 29, 1958).

3. Hansen, M., H. D. Kessler and D. J. McPherson, "The Titanium-Silicon System," Trans. ASM 44 (1953), 518.

4. Dupraw, W. A., "Determination of Tin in Titanium Alloys," Analytical Chemistry 26 (Oct. 1954), 1642.

5. Domagala, R. F. and D. J. McPherson, "System Zirconium-Oxygen," Trans. AIME 200 (1954), 238.

6. Selwood, P. W., Magnetochemistry, 2 ed. (Interscience Publishers Inc., New York, 1956), 42-44.

7. McPherson, D. J. and M. Hansen, "The System Zirconium-Tin," Trans. ASM 45 (1953), 915.

8. Pietrokowsky, P., "Crystal Structure of Zirconium-Rich Compounds with Silicon and Tin," Contract No. DA-04-495-ORD-18, J.P.L. Progress Report No. 20-170 (March 4, 1952).

9. Nowotny, H. and H. Schachner, "X-ray Investigation of the Zirconium-Tin and Zirconium-Iron Systems," Monatsh. Chem. 84 (1953), 169.

10. McPherson et al., "Phase Diagrams of Zirconium-Base Binary Alloys," Contract No. AT(11-1)-149, Final Report (COO-89), (April 14, 1952), 163.

11. Wallbaum, H. J., "The Systems of the Iron Metals with Titanium, Zirconium, Columbium and Tantalum," Arch. Eisenhüttenw. 14 (1941), 521.

12. Hayes, E. T., A. H. Roberson and W. L. O'Brien, Trans. ASM 43 (1951), 888.

13. Hayes, E. T. et al., op. cit., 904.

14. Jordan, C. B. and P. Duwez, "The Structure of Some Alloys of Zirconium with Iron, Cobalt, and Chromium," Contract No. DA-04-495-ORD-18, J.P.L. Progress Report No. 20-196 (June 16, 1953).

15. Elliott, R. P., private communication.

16. Bates, L. F., Modern Magnetism (Cambridge University Press, London, 1951), 122.